Short-circuit characteristics of superconducting permanent magnet generators for 10 MW wind turbines

Liu, Dong; Song, Xiaowei; Wang, Xuezhou; Elhindi, Mohamed; Hasanov, Urfan; Gou, Xiaofan; Ye, Changqing

DOI
10.1109/TASC.2021.3056996

Publication date
2021

Document Version
Accepted author manuscript

Published in
IEEE Transactions on Applied Superconductivity

Short-Circuit Characteristics of Superconducting Permanent Magnet Generators for 10 MW Wind Turbines

Dong Liu, *Member, IEEE*, Xiaowei Song, *Member, IEEE*, Xuezhou Wang, *Member, IEEE*, Mohamed Elhindi, Urfan Hasanov, *Student Member, IEEE*, Changqing Ye, Xiaofan Gou

***Abstract*—Superconducting permanent magnet generators (SCPMGs) are a potential candidate for 10 MW direct-drive wind turbine applications. This paper presents two 10 MW SCPMG designs using MgB_2 cables for the armature winding and investigates the short-circuit characteristics of the designed SCPMGs. The first part of the results shows that the SCPMGs can double the shear stress of a conventional low-speed permanent magnet (PM) generator (from 65 kPa to 130 kPa) whilst avoiding demagnetization of the PMs in rated-load operation. However, the power factor has to drop to a range of 0.7-0.8. The second part of the results shows that during a sudden three-phase short circuit, the superconducting armature winding is prone to quench and the PMs are likely to be demagnetized in both proposed designs.**

***Index Terms*—Demagnetization, MgB_2, permanent magnet, short circuit, superconducting generator, wind turbine.**

I. Introduction

SUPERCONDUCTING machines are competitive to be applied in 10 MW or larger wind turbines due to their compactness and low weight [1]–[3]. A general design option is that the DC field winding of superconducting generators (SCGs) is superconducting at cryogenic temperature, whereas the AC armature winding is still made of copper wires and operates at room temperature [4]–[7]. Such called partially SCGs have rotating cryostats and require rotating coupling for a satisfying cryogenic environment [8], [9]. The rotating coupling adds more costs and may reduce the reliability of the cryogenic cooling system.

An alternative concept, namely superconducting permanent magnet generators (SCPMGs), has been proposed to eliminate the rotating coupling [10]–[13]. The rotor of an SCPMG is with permanent magnets (PMs) at room temperature which excite the main magnetic field. The stator is with a superconducting (SC) armature winding at cryogenic temperature. The SC armature winding carries a large current and boosts the electrical loading of the generator. The generator size can then be smaller compared with conventional low-speed PM generators. This concept has AC loss challenges in the SC winding but its simple structure increases the feasibility from a different perspective [14]–[16]. Good news is that new SC cables with special architectures, e.g. Roebel HTS cables, stranded multi-filamentary MgB_2 cables, laser-scribing-processed HTS cables, are being developed for effectively suppressing AC losses, and thereby increasing the technical feasibility of SC armature windings [17]–[20].

With the assumption that the AC loss problem could be addressed in the near future, SCPMGs still have critical issues to be addressed. The first issue is the power factor. In normal operation, SCPMGs may have a stronger armature reaction than its main field excitation due to large superconducting currents. The influence of armature reaction is reflected by the power factor. A large armature current takes more advantage of the SC material but leads to a lower power factor. Therefore, different power factors result in different normal-operation performances. The second issue is short circuit characteristics. Due to the large fault current, the SC armature winding may be quenched and the PMs may be demagnetized during a sudden short circuit. These two issues in SCPMGs have not yet been investigated in the literature.

This paper presents two designs for 10 MW SCPMGs and investigates the short-circuit characteristics of the designed SCPMGs. Four performance indicators which are important for wind turbine generators are investigated: 1) influences of power factor variation, 2) demagnetization of PMs under normal operation, 3) quenching of the armature winding during a sudden short circuit, and 4) demagnetization of PMs during a sudden short circuit. The results are obtained through finite element simulations with COMSOL Multiphysics.

II. Design of SCPMGs

The SCPMGs are designed for a 10 MW direct-drive wind turbine. The rated speed is 9.6 rpm and the rated voltage (line to line) is 3300 V. In line with the concept of SCPMGs, two generator designs are presented. The first design applies tooth coils in the SC armature winding, namely the fractional-slot concentrated winding (FSCW) design. The other design

This work is supported in part by the Natural Science Foundation of Jiangsu Province of China under Grant BK20190486, in part by the Fundamental Research Funds for the Central Universities under Grant No. 2018B02114, and in part by the Fundamental Research Funds for the Central Universities under Grant No. 2019B02914.

D. Liu, M. Elhindi and U. Hasanov are with the College of Energy and Electrical Engineering, Hohai University, CN-211100 Nanjing, China. E-mail: dongliu@hhu.edu.cn

X. Song is with Vestas Wind Systems A/S, DK-8200 Aarhus, Denmark.

X. Wang is with the Department of Maritime and Transport Technology, Faculty of Mechanical, Maritime and Materials Engineering, Delft University of Technology, NL-2628CD Delft, Netherlands.

C. Ye is with the College of Internet of Things Engineering, Hohai University, CN-213022 Changzhou, China.

X. Gou is with the College of Mechanics and Materials, Hohai University, CN-211100 Nanjing, China.

This article has been accepted for publication in a future issue of this journal, but has not been fully edited. Content may change prior to final publication. Citation information: DOI 10.1109/TASC.2021.3056996, IEEE Transactions on Applied Superconductivity

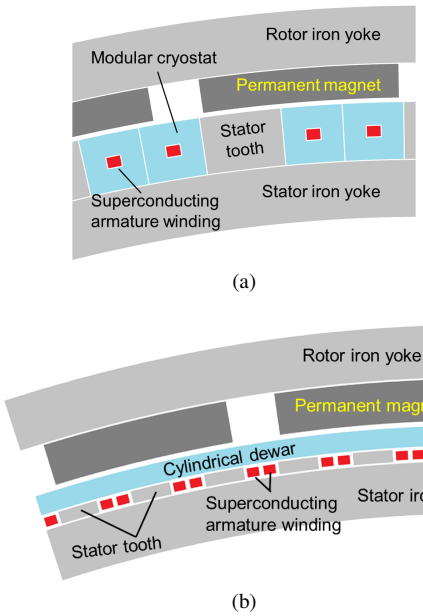

Fig. 1. Sketch of proposed two SCPM designs. (a) FSCW design. (b) ISDW design.

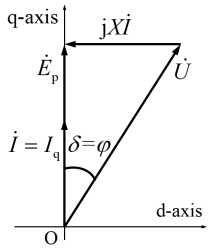

Fig. 2. Phasor diagram of a generator with zero d-axis current control.

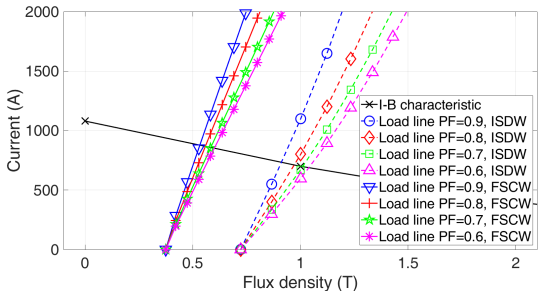

Fig. 3. Load lines and I-B characteristic for determining critical currents of the MgB_2 winding for generator designs with different power factors.

adopts full-pitch coils in the SC armature winding, namely the integral-slot distributed winding (ISDW) design. The numbers of slots per pole per phase are $q = 0.4$ and $q = 1$, respectively.

A. Armature winding

Tooth coils are more feasible than full-pitch coils regarding since the minimum bending radius of a SC wire limits the bending of the end parts of an SC coil. The conventional distributed winding concept seems rather difficult to meet the minimum bending radius, especially short-pitch or double-layer windings [21]. The simplest way to achieve SC windings is still tooth coils in the form of racetrack coils. However, tooth coils produce much more field harmonic contents than full-pitch coils and cause additional losses in the PMs [22]–[24]. Full-pitch coils with $q = 1$ can be made by special end winding bending design to avoid crossing of wires but the imbalance between three phases must be compensated. Then full-pitch coils with $q = 1$ can also be made similar to racetrack coils and comply with the minimum bending radius. However, full-pitch coils with $q > 1$ seem too complicated for coil end bending and are thus not considered.

The adopted SC wires are stranded multi-filamentary MgB_2 cables working at 20 K as presented in [18]. This cable is expected to significantly lower the AC loss level. The generator has an outer rotor with PMs and an inner stator with a MgB_2 armature winding. The bore diameter of the outer rotor is fixed to 5.4 m for both designs. The number of pole pairs is equally 20 for both designs and this number of pole pair makes sufficient space for both two different armature winding arrangements. The number of coils is as low as 48 in the FSCW design. Thus more space of the stator slots enables the use of modular cryostats, i.e. each coil has its own cryostat in the same racetrack shape as shown in Fig. 1a [5], [25]. The three-phase winding arrangement under five poles is: C+c-c-C+a-A+A+a-B+b-b-B+. The distance between the PMs and the armature winding is short. In the ISDW design, the number of coils is 120. Such a large number of coils do not allow modular cryostats, but one conventional cylindrical dewar that encloses the whole stator can apply, as shown in Fig. 1b. The winding arrangement under one pole pair is: A+c-c-B+B+a-a-C+C+b-b-A+. The dewar's wall as well as the thermal insulation parts takes up 40 mm thick and thus significantly increases the distance from the PMs to the armature.

B. Magnetic circuit

The PMs excite the main magnetic field which could be comparative to or lower than the armature reaction field. To increase the main field, the height of the PMs is set to as large as possible. In this design, this height is 80 mm. The width of the PMs is 690.1 mm, 80% of the pole pitch. The stator teeth are made of iron and the slot area should accommodate the MgB_2 coils. For the FSCW design, the slots should be sufficiently high to make space for the modular cryostats. The stator and rotor yokes are made of iron to confine magnetic flux within the generator. The PMs are assumed to be glued onto the rotor iron without changing the magnetic circuit.

C. Control strategy and power factor selection

The rotor is with PMs and thus non-salient. The control strategy of zero d-axis current can be applied due to its simplicity. The armature current is in the quadrature axis and all used to produce torque. In this control strategy, as shown in Fig. 2, the power angle equals the power factor angle. When the armature current increases, the power factor will decrease. If a large current is needed to make better use of the superconductivity, the power factor will become quite low and the amplitude difference between the no-load voltage $\dot{E}_p$ and the rated voltage $\dot{U}$ will become quite large. Therefore,

This article has been accepted for publication in a future issue of this journal, but has not been fully edited. Content may change prior to final publication. Citation information: DOI 10.1109/TASC.2021.3056996, IEEE Transactions on Applied Superconductivity

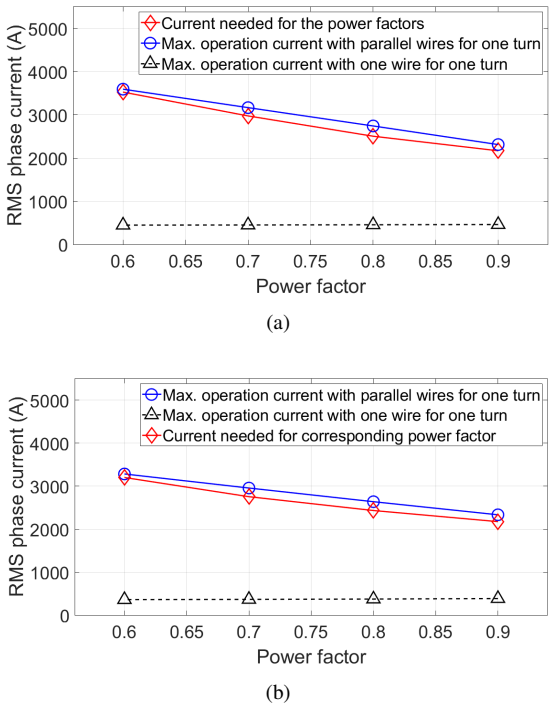

Fig. 4. Needed currents and maximum operation currents of generator designs with different power factors. (a) FSCW design. (b) ISDW design.

four power factors, PF = 0.6, 0.7, 0.8, 0.9, are selected to reflect the levels of the superconducting armature current. The FSCW and ISDW designs with the four power factors will be modeled and compared.

D. Determination of critical and operating currents

According to the I-B critical characteristic of the MgB_2 cable at 20 K, the critical current of the armature winding can be determined by crossing the load lines with the critical characteristic line as shown in Fig. 3. The currents on the load lines are the current amplitude of Phase A. The four power factors give similar load lines and the critical currents are all below 900 A.

The maximum operating current is defined as the RMS current that has a safety margin of 25% below the critical current divided by $\sqrt{2}$. As indicated in Fig. 4, Table I, the phase current needed for each power factor is much larger than the maximum operating current. In other words, one single MgB_2 cable cannot carry the needed current. The proposed solution is to use multiple MgB_2 cables in parallel to form one turn so that the maximum operating current is multiplied to handle the needed phase current. With the use of parallel cables for one turn, the rated RMS current can be achieved. It is assumed here that the critical current of the MgB_2 cable does not change too much by binding multiple cables in parallel. The numbers of parallel MgB_2 cables for one turn are shown in Table I. It is noted that more cables for one turn will make the winding manufacturing much more difficult. The advantage is that the AC loss may be reduced if these parallel cables are appropriately arranged.

The RMS engineering current density in the armature winding is summarized in Table I. The lower power factors result from larger current densities which make more use of the SC material. Compared with the current density of copper, which is usually 3 A/mm^2 for large machines, SC cables can carry about 20-50 times this current density level.

TABLE I
PARAMETERS OF THE FSCW AND ISDW GENERATOR DESIGNS

Power factor (PF)		0.6	0.7	0.8	0.9
Rated power (MW)			10		
Rated speed (rpm)			9.6		
Rated voltage (V)			3300		
Air gap diameter (m)			5.4		
Mech. air gap length (mm)			6		
Mag. air gap length (mm)			46		
No. of pole pairs			20		
No. of slots	FSCW		48		
	ISDW		120		
Rated RMS current (A)	FSCW	3527	2975	2506	2169
	ISDW	3202	2756	2435	2177
Axial stack length (m)	FSCW	1.215	1.491	2.030	3.293
	ISDW	1.066	1.375	1.846	2.828
Critical current (A)	FSCW	847	853	862	872
	ISDW	688	697	711	734
RMS current density (A/mm^2)	FSCW	145	102	73	56
	ISDW	110	81	62	50
No. parallel cables for one turn	FSCW	8	7	6	5
	ISDW	9	8	7	6
End winding inductance (mH)	FSCW	1.100	0.908	0.614	0.284
	ISDW	7.200	5.600	4.000	2.100

E. Shear stress and generator size

The purpose of using superconductivity technology is to boost the torque density or shear stress of a generator. The shear stress of the FSCW and ISDW designs is plotted in Fig. 5 with the four power factors. The axial stack length is also plotted to show the size of the generator. When the armature current is high and the power factor goes to 0.6, the shear stress of the FSCW design approaches 200 kPa while the shear stress of the ISDW design reaches 225 kPa. The stack lengths are 1.215 m and 1.066 m, respectively. When the armature current goes down and the power factor increases, the shear stress of both designs becomes lower. With PF = 0.9, the shear stresses of the two designs become 73 kPa and 85 kPa. It should be noted that the shear stress of a conventional low-speed PM generator is about 65 kPa and the power factor is about PF = 0.92-0.96. To win the battle with the conventional counterpart, an SCPMG needs to double the shear stress of the conventional generator so that the extra cost for superconductivity will be worthwhile. By observing the trends in Fig. 5, the power factors of the FSCW and ISDW designs should go to PF = 0.72-0.78 and PF = 0.74-0.80, respectively. On one hand, these low power factors make more use of the capacity of SC cables. On the other hand, these low power factors require a larger capacity of the power electronic converter for grid connection. As a further comparison, partially SC generators with an SC field winding and a copper armature winding can produce 179 kPa (PF = 1.0) with LTS conductors [9] and 113 kPa (PF = 0.92) with HTS conductors [4].

This article has been accepted for publication in a future issue of this journal, but has not been fully edited. Content may change prior to final publication. Citation information: DOI 10.1109/TASC.2021.3056996, IEEE Transactions on Applied Superconductivity

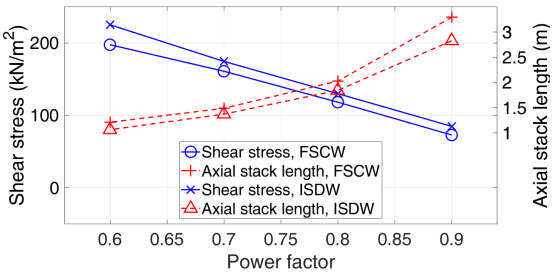

Fig. 5. Shear stresses and axial stack lengths of generator designs with different power factors.

TABLE II
PM DEMAGNETIZED ($\surd$) OR NOT ($\times$) IN RATED-LOAD OPERATION

	Power factor	0.6	0.7	0.8	0.9
FSCW design	$B_{dmg} = 0.3$ T (G1)	$\surd$	$\surd$	$\times$	$\times$
	$B_{dmg} = 0.1$ T (G2)	$\surd$	$\surd$	$\times$	$\times$
	$B_{dmg} = -0.1$ T (G3)	$\surd$	$\times$	$\times$	$\times$
ISDW design	$B_{dmg} = 0.3$ T (G1)	$\surd$	$\surd$	$\times$	$\times$
	$B_{dmg} = 0.1$ T (G2)	$\surd$	$\times$	$\times$	$\times$
	$B_{dmg} = -0.1$ T (G3)	$\times$	$\times$	$\times$	$\times$

F. Demagnetization and permanent magnet grades

Three grades of PMs are selected to examine the demagnetization property of the SCPMGs. The three grades all have a remanence of 1.25 T at 80°C. The lowest grade (G1) starts demagnetization at $B_{dmg} = 0.3$ T which is commonly used in conventional PM generators. The highest grade (G3) starts demagnetization at $B_{dmg} = -0.1$ T which is rather difficult to be demagnetized. The middle grade (G2) has $B_{dmg} = 0.1$ T. The rated-load operation is simulated and checked, and the result is shown in Table II. In both designs, *PF* = 0.9 and *PF* = 0.8 allows to use the G1 PM. With *PF* = 0.7, the FSCW design has to use G3 PM while the ISDW design can use G2 PM. With *PF* = 0.6, the FSCW design has no PM grades to use while the ISDW design can still use G3 PM. This result shows that the FSCW design cannot operate with the power factor of 0.6 due to strong demagnetization.

III. SHORT-CIRCUIT CHARACTERISTICS

After analyzing the shear stress and the rated-load demagnetization of the FSCW and ISDW designs, the power factors of *PF* = 0.7 and *PF* = 0.8 are chosen for the study of short-circuit characteristics. Although *PF* = 0.6 provides impressive high shear stress, it causes strong demagnetization for the FSCW design and elevates the capacity requirement for the power electronic converter. Such high shear stress with a low power factor is not necessary. The high power factor *PF* = 0.9 cannot make the shear stress remarkably higher than that of a conventional PM generator. Therefore, the power factors of 0.6 and 0.9 are not taken into further consideration.

Three-phase short circuits at the armature winding terminal are simulated through field-circuit coupling models with finite element methods [26], [27]. The end winding inductance with each power factor is summarized in Table I. Both no-load and rated-load short circuits are simulated. The short circuit begins when the voltage of Phase A crosses zero so that the short circuit current of Phase A will be maximum.

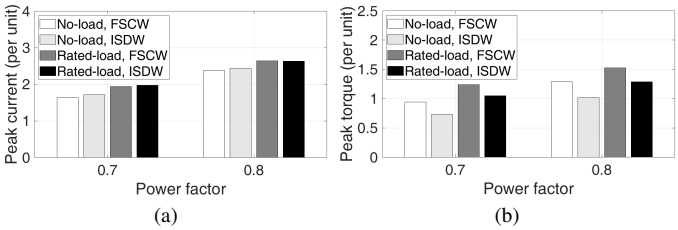

Fig. 6. Peak values of the short-circuit current and torque of generator designs with the two chosen power factors. (a) Peak current. (b) Peak torque.

A. Current and torque

The peak values of short-circuit current and torque of the FSCW and ISDW designs are compared in Fig. 6. Within the same generator design, the higher power factor increases the peak current and peak torque in both the no-load and rated-load short circuits. The FSCW and ISDW designs have similar peak currents but the FSCW design has higher peak torques. The rated-load short circuit leads to a slightly higher current than the no-load short circuit. The torque difference is a bit large between the no-load and rated-load short circuits. However, the peak torque is still under three times the rated torque and will not challenge the shaft strength of a direct-drive wind turbine. The peak currents are all low and below three times the rated current amplitude. From this perspective, both the FSCW and ISDW designs meet the requirements of peak current and peak torque.

B. Examination for quenches

The critical currents in Phase A are calculated through the I-B characteristic of the MgB_2 cable. The maximum norm flux density B in Phase A is retrieved from the finite element solutions and the corresponding critical current I_c is then found. The short-circuit current in Phase A is compared with the critical current. A quench will occur when the short-circuit current exceeds the critical current. It should be noted that the quench is not modeled in the simulation so it does not make any influence on the short circuit process. The quench check results are shown in Fig. 7 for the FSCW design and in Fig. 8 for the ISDW design. In both no-load and rated-load short circuit cases, the phase current exceeds the critical current in the first cycle. The overcurrent is more in the rated-load short circuits. The ISDW design has less overcurrent than the FSCW design. Changing the power factor does not significantly change the extent of overcurrent. This result indicates that a quench is very likely to happen in a three-phase short circuit for both the FSCW and ISDW designs.

C. Examination for demagnetization

In rated-load operation, both the FSCW and ISDW designs have no demagnetization in the PMs with *PF* = 0.7 and 0.8. From the simulation results as shown in Fig. 9, however, both designs have severe demagnetization in the three-phase short circuit even with the highest PM grade (G3, $B_{dmg} = -0.1$ T).

This article has been accepted for publication in a future issue of this journal, but has not been fully edited. Content may change prior to final publication. Citation information: DOI 10.1109/TASC.2021.3056996, IEEE Transactions on Applied Superconductivity

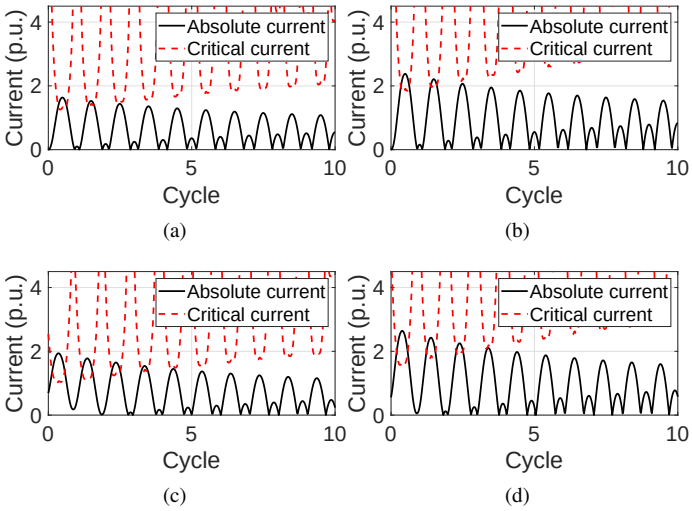

Fig. 7. Short-circuit current in Phase A (in absolute value) compared with critical currents for the FSCW design. (a) PF = 0.7, no-load. (b) PF = 0.8, no-load. (c) PF = 0.7, rated-load. (d) PF = 0.8, rated-load.

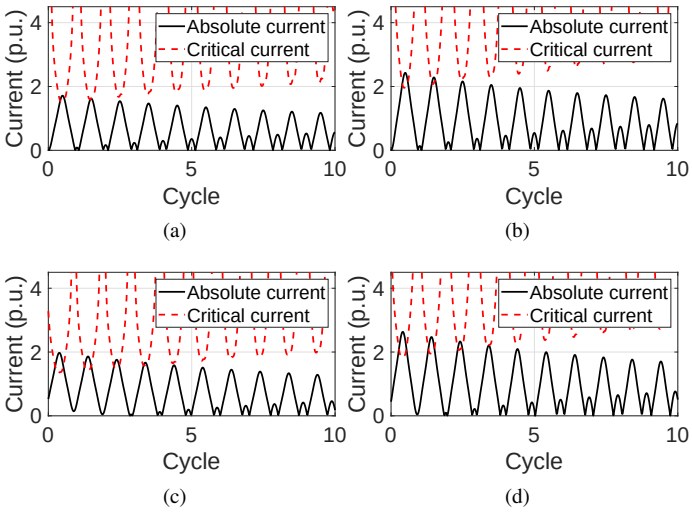

Fig. 8. Short-circuit currents in Phase A (in absolute value) compared with critical currents for the ISDW design. (a) PF = 0.7, no-load. (b) PF = 0.8, no-load. (c) PF = 0.7, rated-load. (d) PF = 0.8, rated-load.

The FSCW design already has heavy demagnetization in the no-load short circuit and a bit more regions of the PMs are demagnetized in the rated-load short circuit. The ISDW design has a slight demagnetization in the no-load short circuit but the demagnetization becomes rather severe in the rated-load short circuit. The lower power factor of 0.7 results in more demagnetization in the rated-load short circuit since the rated armature current is larger and the armature reaction on the PMs is then stronger. This result indicates that demagnetization is very likely to happen in a three-phase short circuit for both the FSCW and ISDW designs even if the PMs already have an excellent anti-demagnetization property.

IV. Conclusion

This paper studies SCPMGs adopting both FSCW and ISDW designs. The findings show that the shear stress in

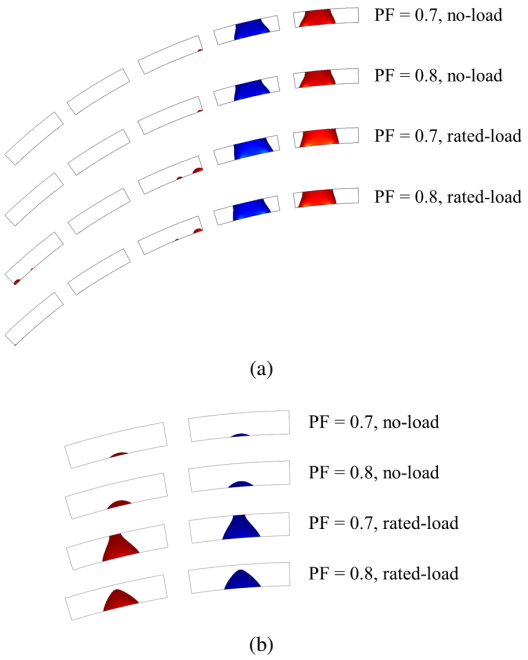

Fig. 9. Demagnetization indicated by colored regions for the two SCPMG designs in the three-phase short circuit, assuming $B_{dmg} = -0.1\ T$. (a) Under five poles, FSCW design. (b) Under one pole pair, ISDW design.

SCPMGs can be as high as 130 kPa, which is doubling the shear stress of a conventional low-speed PM generator (about 65 kPa). However, the power factor has to drop to the range of 0.7-0.8. Such power factors ensure that demagnetization does not occur in rated-load operation if the PM grade is properly selected.

The three-phase short circuit analysis shows that the designed SCPMGs, either FSCW or ISDW, are prone to quench and demagnetization although their fault currents and torques remain acceptably low. Quenches already occur in the first cycle after the short circuit begins with both PF = 0.7 and PF = 0.8. The rated-load short circuits lead to a more excessive phase current over the critical current than the no-load short circuits. The FSCW design has more severe over-current than the ISDW design. The quench may not last long but special action must be taken to protect the superconducting cables. Demagnetization occurs in both the FSCW and ISDW designs even if the PMs already have an excellent anti-demagnetization property ($B_{dmg} = -0.1$ T). With either PF = 0.7 or PF = 0.8, demagnetization occurs in both the no-load and rated-load short circuits.

Under the SCPMG concept, a high power factor, e.g. 0.9, does not provide a competitive shear stress for effectively reducing the size of the generator. The power factor between 0.7-0.8 well utilizes the superconductor's capacity. However, generator size reduction using such low power factors will probably not be accepted by a direct-drive wind power conversion system. Moreover, quenches and demagnetization during a sudden short circuit are unacceptable too. Further studies are still needed to find out how to avoid quenches and demagnetization during a sudden short circuit by means of special design measures whilst maintaining a high shear stress capability and an acceptable power factor.

REFERENCES

[1] K. S. Haran et al., "High power density superconducting rotating machinesdevelopment status and technology roadmap," *Supercond. Sci. and Techno.*, vol. 30, pp. 123002, 2017.

[2] B. B. Jensen, N. Mijatovic, and A. B. Abrahamsen, "Development of superconducting wind turbine generators," *Journal of Renewable and Sustainable Energy*, vol. 5, pp. 023137, 2013.

[3] H. Polinder, J. A. Ferreira, B. B. Jensen, A. B. Abrahamsen, K. Atallah, and R. a. McMahon,"Trends in wind turbine generator systems," *IEEE J. Emerg. Sel. Top. Power Electron.*, vol. 1, pp. 174185, 2013.

[4] X. Song et al., "Designing and Basic Experimental Validation of the World's First MW-Class Direct-Drive Superconducting Wind Turbine Generator," *IEEE Trans. Energy Convers.*, vol. 34, no. 4, pp. 22182225, Dec. 2019.

[5] I. Marino et al.,"Lightweight MgB_2 superconducting 10 MW wind generator," *Supercond. Sci. Technol.*, vol. 29, Feb. 2016, Art. no. 024005.

[6] D. Liu, H. Polinder, A. B. Abrahamsen and J. A. Ferreira, " Topology comparison of superconducting generators for 10-MW direct-drive wind turbines: cost of energy based," *IEEE Trans. Appl. Supercond.*, vol. 27, no. 4, Jun. 2017, Art. No. 5202007.

[7] Ronghai Qu, Yingzhen Liu and Jin Wang, "Review of superconducting generator topologies for direct-drive wind turbines," *IEEE Trans. on Appl. Supercond.*, vol. 23, pp. 5201108, June 2013.

[8] S. S. Kalsi, "Rotating AC Machines," in Applications of High Temperature Superconductors to Electric Power Equipment, IEEE, 2011.

[9] R. Fair et al., "Superconductivity for large scale wind turbines," U.S. DOE report DE-EE0005143, Apr. 2012.

[10] K. Zhang, X. Huang, L. Wu, Y. Fang and W. Cao, "Stator design aspects for permanent magnet superconducting wind power generators," *IEEE Trans. Appl. Supercond.*, vol. 29, no. 2, pp. 1-5, March 2019, Art no. 5201205.

[11] X. Huang, K. Zhang, L. Wu, Y. Fang and Q. Lu, "Design of a dual-stator superconducting permanent magnet wind power generator with different rotor configuration," IEEE Trans. Magnetics, vol. 53, no. 6, pp. 1-4, June 2017, Art no. 8700204.

[12] X. Huang, C. Zhou, K. Zhang, L. Wu, J. Zhang and W. Cao, "Comparison of electromagnetic performance of SCPM wind power generators with different topologies," *IEEE Trans. Appl. Supercond.*, vol. 29, no. 2, pp. 1-5, March 2019, Art no. 5201405.

[13] X. Li, F. Shen, S. Yu and Z. Xue, "Flux-regulation principle and performance analysis of a novel axial partitioned stator hybrid-excitation flux-switching machine using parallel magnetic circuit," *IEEE Transactions on Industrial Electronics*, Early Access.

[14] D. Liu et al., "Ripple field AC losses in 10-MW wind turbine generators with a MgB_2 superconducting field winding," *IEEE Trans. Appl. Supercond.*, vol. 26, no. 3, April 2016, Art no. 5204205.

[15] N. Magnusson, A. B. Abrahamsen, D. Liu, M. Runde and H. Polinder, "Hysteresis losses in MgB_2 superconductors exposed to combinations of low AC and high DC magnetic fields and transport currents," Physica C., vol. 506, pp. 133-137, 2014.

[16] M. Zhang, W. Yuan, J. Kvitkovic and S. Pamidi, "Total AC loss study of 2G HTS coils for fully HTS machine applications," *Supercond. Sci. and Techno.*, vol. 28, no. 11, Art no. 115011, 2015.

[17] W. Goldacker et al., "Roebel cables from REBCO coated conductors: a one-century-old concept for the superconductivity of the future," *Supercond. Sci. and Techno.*, vol. 27, pp. 1-16, 2014, Art no. 093001.

[18] S. S. Kalsi, "Superconducting wnd turbine generator employing MgB_2 windings both on rotor and stator," *IEEE Trans. Appl. Supercond.*, vol. 24, no. 1, pp. 47-53, Feb. 2014, Art no. 5201907.

[19] T. Hoang, L. Quval, C. Berriaud and L. Vido, "Design of a 20-MW fully superconducting wind turbine generator to minimize the levelized cost of energy," *IEEE Trans. Appl. Supercond.*, vol. 28, no. 1, June 2018, Art no. 5206705.

[20] K. Suzuki et al., "Development of a laser scribing process of coated conductors for the reduction of AC losses," *Supercond. Sci. and Techno.*, vol. 20, no. 8, pp. 822826, 2007.

[21] P. Masson et al., "Development of a 3D sizing model for all-superconducting machines for turbo-electric aircraft propulsion," *IEEE Trans. Appl. Supercond.*, vol. 23, no. 3, Jan. 2013, Art no. 3600806.

[22] A. Jassal, H. Polinder and J. A. Ferreira, "Literature survey of eddy-current loss analysis in rotating electrical machines," *IET Electric Power Applications*, vol. 6, no. 9, pp. 743-752, November 2012.

[23] J. Ji et al., "Effect of circumferential segmentation of permanent magnets on rotor loss in fractional-slot concentrated-winding machines," *IET Electric Power Applications*, vol. 11, no. 7, pp. 1151-1159, 2017.

[24] X. Li, X. Wang and S. Yu, "Design and analysis of a novel transverse-flux tubular linear switched reluctance machine for minimizing force ripple," *IEEE Transactions on Transportation Electrification*, Early Access.

[25] A. Bergen et al., "Design of in-field testing of the world's first ReBCO rotor for a 3.6 MW wind generator," *Supercond. Sci. and Techno.*, vol. 32, no. 12, Art. No. 125006, 2019.

[26] X. Song et al., "Short circuit of a 10-MW high-temperature superconducting wind turbine generator," *IEEE Trans. Appl. Supercond.*, vol. 27, no. 4, Jun. 2017, Art. No. 5201505.

[27] Z. Huang, A. Zhao, X. Huang, B. Zhu, Y. Jiang and Z. Jin, "Short-circuit fault simulations in an HTS wind generator with different mechanical conditions," *IEEE Trans. Appl. Supercond.*, vol. 28, no. 3, pp. 1-6, April 2018, Art no. 5204606.